A pitfall in applying non-anticommuting γ_5 in $q\bar{q} \to ZH$ amplitudes

Taushif Ahmed⋆

Dipartimento di Fisica and Arnold-Regge Center, Università di Torino,
and INFN, Sezione di Torino, Via Pietro Giuria 1, I-10125 Torino, Italy

⋆ taushif.ahmed@unito.it

*15th International Symposium on Radiative Corrections:
Applications of Quantum Field Theory to Phenomenology,
FSU, Tallahasse, FL, USA, 17-21 May 2021*

Abstract

In computing the two-loop QCD corrections to a class of Feynman diagrams for the process $q\bar{q} \to ZH$ in Higgs effective field theory, we discover a striking phenomenon. We find the need for an additional local composite operator in the renormalised Lagrangian while employing a non-anticommuting γ_5 in dimensional regularisation. The computation using anticommuting γ_5, however, does not require any such amendment.

Check for updates

1 Introduction

In exploration of the discovered scalar resonance at the Large Hadron Collider, the VH events play an important role. The recent event of the direct observation [1, 2] of the Higgs boson decay to a pair of bottom quarks gets its primary contribution from the VH channel. Owing to its high phenomenological importance, there has been a lot of computations aiming to make the theoretical predictions more precise [3–12]. In this article, we compute the two-loop QCD corrections to the production of the scalar Higgs boson in association with the neutral massive vector boson through quark annihilation in Higgs effective field theory. Through this computation, we discover a striking phenomenon. Employing non-anticommuting γ_5 in dimensional regularisation fails to generate the amplitude fulfilling the expected chiral invariance and Ward identity. The restoration of these essential properties demands amendment of a four-point local composite operator to the renormalised Lagrangian. On the other hand, applying anticommuting γ_5 gives rise to expected results satisfying these criteria.

In the Higgs effective field theory (HEFT), where the top quark loop is integrated out by treating its mass (m_t) infinitely large, the interacting Lagrangian density relevant for the single

scalar Higgs boson production reads as

$$\mathcal{L}_{\text{heff}} = -\frac{1}{4} c_t C_H \frac{H}{v} G^a_{\mu\nu} G^{a,\mu\nu}, \tag{1}$$

where $G^a_{\mu\nu}$, H, v and C_H denote the gluon field strength tensor, scalar Higgs boson, vacuum expectation value of the Higgs field and Wilson coefficient, respectively. We are interested in the massless QCD corrections to third order to the production of a massive neutral vector boson, Z, and the H through quark annihilation within the HEFT, i.e.

$$q(p_1) + \overline{q}(p_2) \rightarrow Z(q_1) + H(q_2), \tag{2}$$

where $q(\overline{q})$ denotes a quark (anti-quark). The four-momenta appearing inside the parentheses satisfy the on-shell conditions $p_1^2 = p_2^2 = 0$ and $q_1^2 = m_Z^2$, $q_2^2 = m_H^2$ with m_Z and m_H being the mass of Z and H boson, respectively.

In the original theory, the two-loop corrections proportional to top-Higgs Yukawa coupling λ_t can be classified into two categories: class-I and class-II, depending on whether the Z boson couples to the external light or the top quark loop, giving rise to different electroweak coupling factors. In (1), the presence of a dimensionless parameter c_t with unit value signifies that we are restricting ourselves to the class-I within HEFT, as shown in figure 1. In ref. [4],
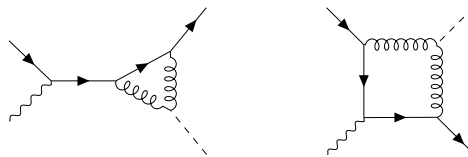
Figure 1: Sample diagrams at the leading order in HEFT. The external curly and dotted lines respectively denote the Z and H-bosons.

it was demonstrated through heavy-mass expansion to class-I, that the leading term in $1/m_t$ does not involve the effective vertex $q\overline{q}ZH$ or $q\overline{q}H$. Consequently, the leading approximation can equivalently be captured through the aforementioned effective Lagrangian (1) where H couples to only gluons. *Through this article*, we will discover that the validity of this statement depends on how we regularise the axial current, depending on whether we adopt an anticommuting or non-anticommuting γ_5, the statement holds true or fails, respectively. We start by computing the quantum loop corrections to this process using anticommuting γ_5 in the next section.

2 Form factors employing anticommuting γ_5

The amplitude $\mathcal{A}$ can be decomposed into vector ($\mathcal{A}_{vec}$) and axial ($\mathcal{A}_{axi}$) parts as

$$\mathcal{A} = c_t\, g_{V,q}\, \bar{v}(p_2) \Gamma^\mu_{vec} u(p_1) \varepsilon^*_\mu(q_1) + c_t\, \bar{v}(p_2) \Gamma^\mu_{axi} u(p_1) \varepsilon^*_\mu(q_1) \equiv c_t\, g_{V,q}\, \mathcal{A}_{vec} + c_t\, \mathcal{A}_{axi}, \tag{3}$$

where we have factored out the vector coupling $g_{V,q}$ between the Z boson and light quark. The polarisation vector of the Z boson is denoted by ε_μ. By performing the Lorentz covariance decomposition of $\mathcal{A}_{vec}$ in terms of linearly independent and complete Lorentz structures in D($= 4-2\epsilon$)-dimensions as

$$\mathcal{A}^\mu_{vec} = \bar{v}(p_2) \big(\mathcal{F}_{1,vec} \slashed{q}_1 p_1^\mu + \mathcal{F}_{2,vec} \slashed{q}_1 p_2^\mu + \mathcal{F}_{3,vec} \slashed{q}_1 q_1^\mu + \mathcal{F}_{4,vec} \gamma^\mu \big) u(p_1). \tag{4}$$

While performing the decomposition, we make sure the chirality is conserved along the massless quark line. From the tensorial structures present in (4), we can construct a set of four projectors in D-dimensions which can subsequently be applied on the set of Feynman diagrams to compute the form factors (FF) $\mathcal{F}_{i,vec}$ order by order in perturbation theory.
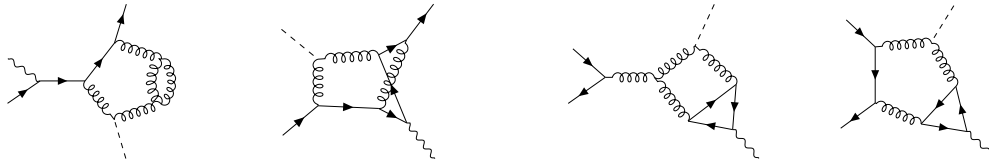
Figure 2: Sample non-singlet (first two) and singlet (last two) diagrams at the next-to-leading order in HEFT

The axial part of the amplitude can further be categorised into non-singlet ($\mathcal{A}_{axi(ns)}$) and singlet ($\mathcal{A}_{axi(s)}$) components as

$$\mathcal{A}_{axi} = g_{A,q} \, \mathcal{A}_{axi(ns)} + g_{A,b} \, \mathcal{A}_{axi(s)} . \tag{5}$$

Through figures 1 and 2, we show some sample Feynman diagrams at one- and two-loop. The singlet diagrams, featuring a closed fermionic triangle loop and exhibiting anomalous behaviour, start appearing from two-loop. By performing a Lorentz covariant decomposition of the axial part, we get

$$\mathcal{A}_{axi}^{\mu} \equiv \bar{v}(p_2) \left(\mathcal{F}_{1,axi} \slashed{q}_1 p_1^{\mu} + \mathcal{F}_{2,axi} \slashed{q}_1 p_2^{\mu} + \mathcal{F}_{3,axi} \slashed{q}_1 q_1^{\mu} + \mathcal{F}_{4,axi} \gamma^{\mu} \right) \gamma_5 u(p_1) . \tag{6}$$

The computation of the non-anomalous part $\mathcal{A}_{axi(ns)}$, which gets translated to the computations of $\mathcal{F}_{i,axi(ns)}$, is performed using anticommuting γ_5^{AC} in D-dimensions. Due to the presence of axial anomaly, we calculate the $\mathcal{F}_{i,axi(s)}$ adopting non-anticommuting γ_5 which we discuss in the next section. By performing the strong coupling constant and operator renormalisation of (1), we arrive at the ultraviolet (UV) finite set of FF to two loops which are found to contain the soft and collinear (IR) divergences, as predicted through the universal subtraction operators [13]. Moreover, we find that the finite remainders ($\epsilon \to 0$) of the FF satisfy

$$\mathcal{F}_{i,axi(ns)}^{(l)} = \mathcal{F}_{i,vec}^{(l)} , \quad i = 1,2,3,4 , \quad l = 1,2 , \tag{7}$$

with

$$\mathcal{F}_{i,va} = \sum_{l=1}^{\infty} a_s^{(l+1)}(\mu_R) \mathcal{F}_{i,va}^{(l)} , \quad va = vec, axi(ns) . \tag{8}$$

$a_s(\mu_R) \equiv \alpha_s(\mu_R)/(4\pi)$ is the strong coupling constant at the renormalisation scale μ_R. The identity in (7) is a reflection of the expected chiral invariance. Our method of computation is presented in refs. [12, 14]. We discuss the computation by employing the non-anticommuting γ_5 in the following section where we encounter a technical pitfall starting from the leading order (LO) itself.

3   Form factors employing non-anticommuting γ_5 in HEFT

The non-anticommuting (NAC) γ_5 can be defined in terms of Dirac's γ^{μ} matrix in dimensional regularisation as [15, 16]

$$\gamma_5 = -\frac{i}{4!} \varepsilon_{\mu\nu\rho\sigma} \gamma^{\mu} \gamma^{\nu} \gamma^{\rho} \gamma^{\sigma} , \tag{9}$$

where the Lorentz indices of the Levi-civita symbol $\varepsilon_{\mu\nu\rho\sigma}$ are treated in D dimensions [17]. Owing to the usage of this definition, UV renormalisation requires an additional treatment [18] to ensure the restoration of the appropriate Ward identity. However, while verifying the expected Ward identity, we discover a striking phenomenon. Although the finite remainders ($\epsilon \to 0$) of the LO vector form factors are identical to the corresponding quantities obtained using AC γ_5, the axial ones are not. In particular, we find that

$$\mathcal{F}^{(1),\text{NAC}}_{i,axi(ns)} = \mathcal{F}^{(1)}_{i,vec}, \quad i = 1, 2, 3,$$
$$\mathcal{F}^{(1),\text{NAC}}_{4,axi(ns)} \neq \mathcal{F}^{(1)}_{4,vec}. \tag{10}$$

Throughout this article, we append AC and NAC for denoting the respective γ_5 scheme. The above inequality implies the violation of the Ward identity even at the LO level

$$q_{1,\mu} \mathcal{A}^{\mu,\text{NAC}}_{axi(ns)} \neq 0. \tag{11}$$

The restoration of the Ward identity, which is a necessity, demands an amendment term of the form

$$\mathcal{J}^{\mu,\text{NAC}} \equiv Z^h_5(a_s) \mathbf{C}\left(\bar{v}(p_2) [\gamma^\mu \gamma_5]_L u(p_1)\right). \tag{12}$$

The constant factor $\mathbf{C} \equiv a_s (-4C_F) C_H/v$ collects the overall a_s^2 of the LO amplitude and $[\gamma^\mu \gamma_5]_L$ implies the axial vector current is renormalised according to Larin's scheme [17,18]. Of course, this renormalisation starts playing a role from the next-to-LO (NLO). The additional renormal-
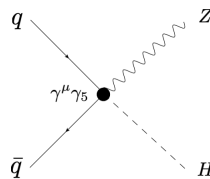
Figure 3: The amendment vertex to the Lagrangian for using NAC in HEFT

isation constant $Z^h_5(a_s) = 1 + \mathcal{O}(a_s)$ that is introduced in the amendment term must be determined order by order in perturbation theory. In the upcoming subsection, we demonstrate this at the NLO. This amendment term can be visualised as a four-point local composite operator as shown in figure 3. With this extra term, we restore the desired properties: $\mathcal{F}^{(1),\text{NAC}}_{i,axi(ns)} = \mathcal{F}^{(1)}_{i,vec}$ holds for all four FF and consequently $q_{1,\mu} \mathcal{A}^{\mu,\text{NAC}}_{axi(ns)} = 0$ is also fulfilled at the LO.

The discrepancy is found to arise solely from the box diagram in figure 1. Although each of the diagrams at the LO is individually finite, the box consists of separately diverging terms. Usage of the NAC and AC schemes of γ_5 gives rise to different D dependent coefficients of these diverging terms, which results in some non-vanishing evanescent anti-commutators upon shifting the non-anticommutating γ_5 from inside the loop to the outside. This leads to the observed discrepancy.

3.1 UV Renormalisation of non-anomalous diagrams at the NLO

At the NLO, we have non-singlet (non-anomalous) as well as singlet (anomalous) set of diagrams, as shown in figure 2. From our experience with the LO, it is quite expected that the phenomenon shows up even at the NLO. For non-anomalous diagrams, the normal form of the Ward identity should hold for the axial current, exactly same as the vector counterpart. We find that the axial form factors renormalised according to Larin's prescription [17,18] exhibit the following behaviours:

1. the IR pole structure, in particular, the single pole in ϵ, differs from the universal prediction [13],

2. the $\mathcal{O}(\epsilon^0)$ term obtained after IR subtraction fails to satisfy the Ward identity.

These shortcomings can be cured by incorporating the quantum loop corrections to the amendment vertex (12). By demanding the restoration of the aforementioned properties, we get

$$Z_{5,ns}^h(a_s) = 1 + a_s \left(\frac{-\beta_0}{\epsilon} + \frac{107}{18}C_A - 7C_F - \frac{1}{9}n_f \right) + \mathcal{O}(a_s^2), \tag{13}$$

where $\beta_0 = 11C_A/3 - 2n_f/3$ is the leading coefficient of the QCD β-function, C_A and C_F are respectively the quadratic Casimirs in adjoint and fundamental representations, n_f is the number of active light quark flavours. To summarise, the renormalised non-singlet axial amplitude $\mathcal{A}_{axi(ns)}$ in HEFT employing NAC γ_5 is given by

$$\mathcal{A}_{axi(ns)}^{\mu,\text{NAC}}(a_s) = Z_{5,L}^{ns}(a_s)Z_{A,L}^{ns}(a_s)Z_H(a_s)\hat{\mathcal{A}}_{axi(ns)}^{\mu,\text{NAC}}(\hat{a}_s) + \mathcal{J}_{ns}^{\mu,\text{NAC}} \tag{14}$$

with the counterterm involving the amendment

$$\begin{aligned} \mathcal{J}_{ns}^{\mu,\text{NAC}} &= Z_{5,ns}^h(a_s)\mathbf{C}\left(\bar{v}(p_2) \, [\gamma^\mu\gamma_5]_L \, u(p_1) \right) \\ &= Z_{5,ns}^h(a_s)Z_{5,L}^{ns}(a_s)Z_{A,L}^{ns}(a_s)\mathbf{C}\left(\bar{v}(p_2) \, \gamma^\mu\gamma_5 \, u(p_1) \right). \end{aligned} \tag{15}$$

The renormalisation constants for the non-singlet axial currents in Larin scheme are encoded through $Z_{A,L}^{ns}$ and $Z_{5,L}^{ns}$ [18]. We denote the operator renormalisation for (1) by Z_H. The symbol hat(ˆ) is used to indicate the bare amplitude that we get directly from Feynman diagrams. If we choose not to invoke the Larin counterterms in (15), we could only determine the product $Z_{5,ns}^{h,\text{T}}(a_s) \equiv Z_{5,ns}^h(a_s)Z_{5,L}^{ns}(a_s)Z_{A,L}^{ns}(a_s)$ as a whole.

3.2 UV Renormalisation of anomalous diagrams

Treatment of the singlet diagrams, as shown in figure 2, is trickier owing to the presence of ABJ anomaly [19, 20]. The only nonzero contribution in singlet diagrams comes from the massless b-quark loop in $n_f = 5$ flavour HEFT, that involves the coupling factor $g_{A,b}c_t$. Other generations of quarks do not contribute due to the mass degeneracy. The ABJ anomaly of the massless axial vector b-quark current $J_{5\mu} = \bar{b}\gamma_\mu\gamma_5 b$ at the operator level reads as

$$\left[\partial^\mu J_{5\mu} \right]_R = a_s \frac{1}{2}\left[G\tilde{G} \right]_R, \tag{16}$$

where $G\tilde{G} = -\epsilon^{\mu\nu\rho\sigma}G_{\mu\nu}^a G_{\rho\sigma}^a$. We put the subscript R to signify the relation holds for renormalised operators [18, 21]. The divergence of $J_{5\mu}$ gets translated to the replacement $\varepsilon_\mu^* \to q_{1,\mu}$. At the matrix element level in momentum space, we get

$$\mathcal{A}_{axi(s)}^\mu q_{1,\mu} = \frac{a_s}{2}\left\langle H(q_2) \middle| \left[G\tilde{G}(0) \right]_R \middle| q(p_1)\bar{q}(p_2) \right\rangle \tag{17}$$

obeying the kinematic relation $p_1 + p_2 - q_2 = q_1$. The above Green's function has an insertion of the composite operator $\left[G\tilde{G}(0) \right]_R$ with momentum q_1^μ. Note that, the l.h.s. as well as the r.h.s. is individually finite. By computing the r.h.s. in perturbation theory, for which some diagrams are shown in figure 4, we find that the relation (17) fails to hold true. In view of our treatment for non-anomalous diagrams at the NLO, we introduce the local composite operator

$$\mathcal{J}_s^{\mu,\text{NAC}} = Z_{5,s}^h(a_s)\mathbf{C}\left(\bar{v}(p_2) \, [\gamma^\mu\gamma_5]_L \, u(p_1) \right) \tag{18}$$
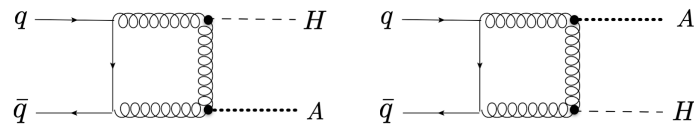
Figure 4: Diagrams contributing to the right-hand side of (17). The blobs denote the effective vertex.

with a new undetermined renormalisation constant $Z_{5,s}^h(a_s)$. By demanding the finite anomaly and restoration of the anomalous Ward identity (16) or (17), we obtain

$$Z_{5,s}^h(a_s) = 1 + a_s \left(-\frac{3}{2}\frac{1}{\epsilon} - \frac{3}{4} \right) + \mathcal{O}(a_s^2). \tag{19}$$

In the process of renormalising the matrix elements on the r.h.s. of (17), we require the following mixed counterterm

$$Z_{GJ}^h(a_s)\big(\bar{v}(p_2)\gamma_\mu\gamma_5 u(p_1)q_1^\mu\big) \tag{20}$$

where $Z_{GJ}^h(a_s) = a_s \left(\frac{24}{\epsilon}C_F \right) + \mathcal{O}(a_s^2)$ is determined to minimally subtract all the poles in figure 4.

To summarise, the renormalised effective Lagrangian with a non-anticommuting γ_5 for computing the class-I diagrams of $q\bar{q} \to ZH$ in HEFT reads as

$$\mathcal{L}_R = \Big[\mathcal{L}_c + \mathcal{L}_{\text{heff}} \Big]_R + \kappa\, Z_5^h(a_s)\mathbf{C}\Big(\bar{q}_R(x)\,[\gamma^\mu\gamma_5]_L\, q_R(x)\Big)Z_\mu(x)H(x), \tag{21}$$

where $\kappa_{ns} = c_t g_{A,q}$ and $\kappa_s = c_t g_{A,b}$. The first term is the renormalised Lagrangian without the new amendment, as captured through the second term. The latter does not arise while computing the QCD corrections to non-anomalous set of diagrams employing the anticommuting γ_5 scheme.

3.3 Form factors in exact theory without heavy-top limit

To make our understanding more concrete, we intend to examine whether the need of the additional local composite operator persists in the full theory with $n_f = 6$ while using non-anticommuting γ_5. We have 6 Feynman diagrams at two-loop with a finite top mass, with
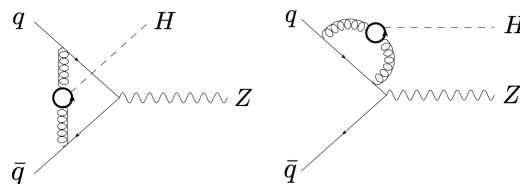
Figure 5: Sample diagrams of the two-loop class-I which are proportional to λ_t. The thick solid lines denote the massive top quark.

samples shown in figure 5. We generate the integrand using GoSam [22, 23] and apply the integration-by-parts [24, 25] relations employing Kira [26] to express the bare amplitude in terms of 55 master integrals. Using pySecdec [27], we evaluate the integrals numerically at one chosen kinematic point as this is sufficient for our purpose. We find that the vector and axial form factors of the two-loop class-I diagrams indeed are identical to each other without the need of any amendment to the Lagrangian. In particular, the 4-th vector and axial FF

agree to the fourth significant digit. Therefore, although we need to introduce an effective four-point vertex in HEFT while working with a non-anticommuting γ_5, we do not need to do so in the exact theory with $n_f = 6$.

4 Conclusion

Our exploration with the class-I diagrams in HEFT ($n_f = 5$) shows that the correct results obeying the chiral invariance as well as the appropriate Ward identity can be obtained for the vector and non-anomalous axial amplitude with anticommuting γ_5. However, for non-anticommuting γ_5, we need an additional four-point effective vertex $q\gamma_\mu\gamma_5\bar{q}Z^\mu H$. In the exact theory with $n_f = 6$ flavours, we do not need any additional composite operator of this kind despite using non-anticommuting γ_5. This observation strengthens the common lore that a conclusion obtained employing anticommuting γ_5 does not necessarily holds for non-anticommuting γ_5 in dimensional regularisation. For which class of processes the need of this kind of effective operator arises is an interesting arena that we intend to explore in months.

Acknowledgements

The author, together with Werner Bernreuther, Long Chen, and Michał Czakon thank the organisers of RADCOR-LoopFest 2021.

Funding information The author received funding from the European Research Council (ERC) under the European Union's Horizon 2020 research and innovation programme *High precision multi-jet dynamics at the LHC* (ERC Condsolidator grant agreement No 772009).

References

[1] M. Aaboud et al., *Observation of $H \to b\bar{b}$ decays and VH production with the ATLAS detector*, Phys. Lett. B **786**, 59 (2018), doi:10.1016/j.physletb.2018.09.013.

[2] A. M. Sirunyan *et al.*, *Observation of Higgs boson decay to bottom quarks*, Phys. Rev. Lett. **121**, 121801 (2018), doi:10.1103/PhysRevLett.121.121801.

[3] O. Brein, A. Djouadi and R. Harlander, *NNLO QCD corrections to the Higgs-strahlung processes at hadron colliders*, Phys. Lett. B **579**, 149 (2004), doi:10.1016/j.physletb.2003.10.112.

[4] O. Brein, R. V. Harlander, M. Wiesemann and T. Zirke, *Top-quark mediated effects in hadronic Higgs-Strahlung*, Eur. Phys. J. C **72**, 1868 (2012), doi:10.1140/epjc/s10052-012-1868-6.

[5] G. Ferrera, M. Grazzini and F. Tramontano, *Associated ZH production at hadron colliders: The fully differential NNLO QCD calculation*, Phys. Lett. B **740**, 51 (2015), doi:10.1016/j.physletb.2014.11.040.

[6] T. Ahmed, M. Mahakhud, N. Rana and V. Ravindran, *Drell-Yan production at threshold to third order in QCD*, Phys. Rev. Lett. **113**, 112002 (2014), doi:10.1103/PhysRevLett.113.112002.

[7] Y. Li, A. von Manteuffel, R. M. Schabinger and H. Xing Zhu, *N³LO Higgs boson and Drell-Yan production at threshold: The one-loop two-emission contribution*, Phys. Rev. D **90**, 053006 (2014), doi:10.1103/PhysRevD.90.053006.

[8] S. Catani, L. Cieri, D. de Florian, G. Ferrera and M. Grazzini, *Threshold resummation at N³LL accuracy and soft-virtual cross sections at N³LO*, Nucl. Phys. B **888**, 75 (2014), doi:10.1016/j.nuclphysb.2014.09.012.

[9] M. C. Kumar, M. K. Mandal and V. Ravindran, *Associated production of Higgs boson with vector boson at threshold N³LO in QCD*, J. High Energy Phys. **03**, 037 (2015), doi:10.1007/JHEP03(2015)037.

[10] J. M. Campbell, R. Keith Ellis and C. Williams, *Associated production of a Higgs boson at NNLO*, J. High Energy Phys. **06**, 179 (2016), doi:10.1007/JHEP06(2016)179.

[11] G. Ferrera, G. Somogyi and F. Tramontano, *Associated production of a Higgs boson decaying into bottom quarks at the LHC in full NNLO QCD*, Phys. Lett. B **780**, 346 (2018), doi:10.1016/j.physletb.2018.03.021.

[12] T. Ahmed, A. H. Ajjath, L. Chen, P. K. Dhani, P. Mukherjee and V. Ravindran, *Polarised amplitudes and soft-virtual cross sections for $b\bar{b} \to ZH$ at NNLO in QCD*, J. High Energy Phys. **01**, 030 (2020), doi:10.1007/JHEP01(2020)030.

[13] S. Catani, *The singular behaviour of QCD amplitudes at two-loop order*, Phys. Lett. B **427**, 161 (1998), doi:10.1016/S0370-2693(98)00332-3.

[14] T. Ahmed, W. Bernreuther, L. Chen and M. Czakon, *Polarized $q\bar{q} \to Z+Higgs$ amplitudes at two loops in QCD: the interplay between vector and axial vector form factors and a pitfall in applying a non-anticommuting γ_5*, J. High Energy Phys. **07**, 159 (2020), doi:10.1007/JHEP07(2020)159.

[15] G. 't Hooft and M. Veltman, *Regularization and renormalization of gauge fields*, Nucl. Phys. B **44**, 189 (1972), doi:10.1016/0550-3213(72)90279-9.

[16] P. Breitenlohner and D. Maison, *Dimensional renormalization and the action principle*, Commun. Math. Phys. **52**, 11 (1977), doi:10.1007/BF01609069.

[17] S. A. Larin and J. A. M. Vermaseren, *The α_s^3 corrections to the Bjorken sum rule for polarized electroproduction and to the Gross-Llewellyn Smith sum rule*, Phys. Lett. B **259**, 345 (1991), doi:10.1016/0370-2693(91)90839-I.

[18] S. A. Larin, *The renormalization of the axial anomaly in dimensional regularization*, Phys. Lett. B **303**, 113 (1993), doi:10.1016/0370-2693(93)90053-K.

[19] S. L. Adler, *Axial-vector vertex in spinor electrodynamics*, Phys. Rev. **177**, 2426 (1969), doi:10.1103/PhysRev.177.2426.

[20] J. S. Bell and R. Jackiw, *A PCAC puzzle: $\pi^0 \to \gamma\gamma$ in the σ model*, Nuov Cim A **60**, 47 (1969), doi:10.1007/BF02823296.

[21] T. Ahmed, L. Chen and M. Czakon, *Renormalization of the flavor-singlet axial-vector current and its anomaly in dimensional regularization*, J. High Energy Phys. **05**, 087 (2021), doi:10.1007/JHEP05(2021)087.

[22] G. Cullen et al., *GOSAM-2.0: a tool for automated one-loop calculations within the Standard Model and beyond*, Eur. Phys. J. C **74**, 3001 (2014), doi:10.1140/epjc/s10052-014-3001-5.

[23] S. Jones, *Automation of 2-loop amplitude calculations*, Proc. Sci. **260**, 069 (2016), doi:10.22323/1.260.0069.

[24] F. V. Tkachov, *A theorem on analytical calculability of 4-loop renormalization group functions*, Phys. Lett. B **100**, 65 (1981), doi:10.1016/0370-2693(81)90288-4.

[25] K. G. Chetyrkin and F. V. Tkachov, *Integration by parts: The algorithm to calculate β-functions in 4 loops*, Nucl. Phys. B **192**, 159 (1981), doi:10.1016/0550-3213(81)90199-1.

[26] P. Maierhöfer and J. Usovitsch, *Kira 1.2 Release Notes*, arXiv:1812.01491.

[27] S. Borowka, G. Heinrich, S. Jahn, S. P. Jones, M. Kerner, J. Schlenk and T. Zirke, *pySecDec: A toolbox for the numerical evaluation of multi-scale integrals*, Comput. Phys. Commun. **222**, 313 (2018), doi:10.1016/j.cpc.2017.09.015.